A Conformational Study on the Algal Polysaccharide Ulvan†

Gaio Paradossi,*,‡ Francesca Cavalieri, and Ester Chiessi‡

Department of Chemical Sciences and Technologies, University of Rome "Tor Vergata", 00133 Rome, Italy, and section B INFM Unità Roma Tor Vergata

Received January 28, 2002; Revised Manuscript Received May 8, 2002

ABSTRACT: The conformational behavior of the algal polysaccharide ulvan in aqueous solution has been studied. This biopolymer, containing limited regular regions of aldobiuronic sequences made of β-D-glcpA-(1→4)-α-L-rhap 3-sulfate and of α-L-idopA(1→4)-α-L-rhap 3-sulfate, can be considered as a low-cost source of rare sugars with a potential impact on several industrial applications, from pharmaceutical to fine chemistry industry. The relationship of structure with the chemical composition of the saccharidic residues in the biopolymer is evidenced with respect to the ability of iduronic acid moiety to assume two main ring conformations, namely the $^1C_4$ chair and the $^2S_0$ skew boat conformations. Experimental results are interpreted in the light of models obtained from conformational analysis calculations.

Introduction

In the past decade marine eutrophication has promoted the prolification of algal biomasses, namely of *Ulva sp*. In this context the issue of innovative exploitation of these algal biomasses has been raised in particular for its polysaccharidic part. The potentialities for this material are manifold spanning from the food industry to pharmaceuticals and biotechnology.[1]

Moreover, the exploitation of this marine biomass can also represent a remedy to related environmental and economical concerns. One of the products easily obtainable from ulvales seaweeds has been known as a polysaccharide, a phycocolloid[2] commonly indicated with the name of ulvan. Studying the saccharidic composition of ulvan, Percival showed that by this name is indicated a family of water-soluble anionic polysaccharides structurally heterogeneous containing galactose, xylose, rhamnose, glucuronic acid, and iduronic acid arranged in an essentially linear fashion.[3] The presence of limited regular sequences has been pointed out later on by Lahaye et al.[4] The composition and extent of these structural motifs, called aldobiuronic A_{3S} and B_{3S} sequences, can vary depending on the sources and on the year period of the collection of the algal material. On ulvan from *U. Armoricana* the aldobiuronic sequences, shown in Chart 1, have been determined combining enzymic degradation and NMR analysis.[5] The aldobiuronic blocks of ulvan are identified as sulfated glucuronorhamnose and iduronorhamnose, arranged in regular sequences in the chain backbone. One of the main features of such polysaccharides is therefore the presence of uncommon sugars as iduronic acid and sulfated rhamnose. Moreover, these blocks have a close similarity with mammalian glycosamminoglycans[6] already used for their antithrombotic activity such as heparin and heparan sulfate. In this respect sulfated marine polysaccharides represent an alternative as substitutes to heparin whose isolation from mammalian sources like bovine intestinal mucosa can be subjected to the risk of contamination with BSE related prions as already documented in the literature.[7] Although the bioactivity properties, i.e., cytoxicity, antiviral activity, and enhancement/inhibition of bacterial growth, of this polysaccharide are still to be unveiled, in food industry ulvan represents a dietary fiber not degraded by human digestive enzymes, and it can be considered a potential new nutraceutical.[8]

Chart 1

A_{3S}

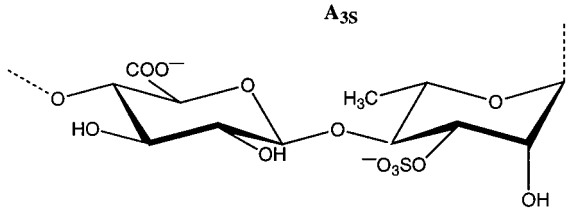

[→4)-β-D-GlcpA-(1→4)-α-L-Rhap3-sulfate-(1→]

B_{3S}

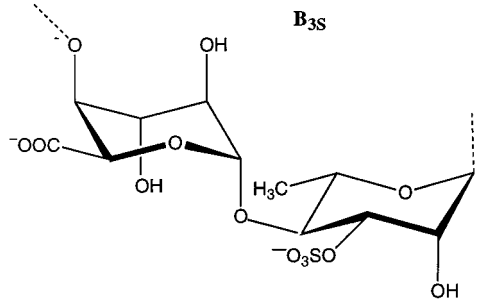

[→4)-α-L-IdopA-(1→4)-α-L-Rhap3-sulfate-(1→]

Ulvan represents the major biopolymeric fraction of the cell wall of *Ulva*, and it is believed to control the osmolar stability of the cell and to maintain a suitable environment and protection of the cell. As is often the case for cell wall polysaccharides, also ulvans are complexed with protein moieties in their native state.

The regular sequences contained in the chain probably participate in the mechanism of formation of a weak gel when ulvan is in the presence of divalent cations or borate.[9,10] It can be also envisaged the possibility that the ulvan conformational state may be influenced by the existence of such regular sequences.

From these considerations it appears clear that the potentiality of ulvan is manifold but yet poorly studied.

† This paper is dedicated to the memory of the late Prof. A. M. Liquori, who inspired us to this subject.

‡ Section B INFM Unità Roma Tor Vergata.

* Corresponding author: e-mail paradossi@stc.uniroma2.it.

10.1021/ma020134s CCC: $22.00
Published on Web 06/29/2002

An investigation on the relationships governing the structural−fuctional properties of this polysaccharide is a prerequisite for any innovative use of ulvales.

In a recent study we focused on the circular dichroism behavior of ulvan from *U. Rigida* in order to understand its conformational properties in relation with the solution and gel state.[11] In this paper we present a study extended on ulvans from other sources and addressed to other properties such as ion binding clearly influenced by the possibility of a disorder-to-order transition.

Experimental Section

Materials. Ulvan samples from different origin were kind gifts of Dr. M. Lahaye of I.N.R.A. (France) and of Dr. Dan of S.I.N.C.O.M. (Italy). Most of the determinations were carried out on ulvan from *Ulva Armoricana*. Other ulvan samples studied for comparative purposes were from *Ulva Lactuca*, *Ulva Rotundata*, and *Ulva Rigida* (from Venice Lagoon, Italy, and France).

Inorganic salts were Carlo Erba products and used without further purification. Strong cationic exchange resin, Amberlite IR-120, was a Merk product.

Milli-Q grade water was produced with a USF Elga apparatus.

Rhamnose, glucose, galactose, xylose, glucuronic acid (Fluka), and galactose amine (Sigma) were used without further purification as standards for HPAEC. Enzymic degradation of the polysaccharide was carried out with *Helix pomatia* β-glucuronidase (Sigma).

Methods. *1. Extraction and Purification.* The dry algal biomass was treated as already described in the literature.[11] Ulvan was stored as a dry powder in sodium salt form.

Elemental analysis carried out with an elemental analyzer EA1108 (Carlo Erba) was used to evaluate the protein nitrogen content after purification which was 0.53% (w/w). This protein impurity was not detected by UV absorption and circular dichroism spectroscopies around 280 nm.

2. Determination of the Repeating Unit Mass per Charge. An aqueous solution of ulvan at a concentration of 3 g/L was run through Amberlite IR-120 resin to obtain the charged polysaccharide in the acid form. Potentiometric titration was carried out with standardized NaOH (0.02 M) by means of a Radiometer Copenhagen pHmeter equipped with a semimicro combined glass electrode (Mettler).

3. Circular Dichroism Spectroscopy. UV spectra, typically in the range 200−300 nm, were recorded with a JASCO J600 dichograph using thermostated quartz cells.

4. Isothermal Microcalorimetry. Isothermal microcalorimetry titrations were carried out with a TAM (Thermometrics). In a typical experiment 2 mL of ulvan solution was placed in a stainless steel cell and added with the titrant by means of a computer-controlled step motor injector delivering 10 μL aliquots. Data collection and treatment were computer assisted.

5. Light Scattering and Osmometry Measurements. A stock solution of ulvan in aqueous 0.1 M NaCl to suppress Donnan effects was diluted to obtained a set of solutions using the same solvent. Solution were filtered through Millipore 0.45 μm filters directly into the cells. The differential refractive index, $(dn/dc)_\mu$, was taken equal to 0.127 mL/g as found for ι-carrageenan.[12] A Brookhaven BI200 photometer equipped with a solid-state laser radiation at 532 nm was used in decalin as refractive index matching liquid. Concentrations from 0.03 to 1 g/L and an angular range from 20° to 154° were explored in each experiments. The excess scattering, of ulvan aqueous solutions in 0.1 M NaCl extrapolated at $\theta = 0$, i.e., the forward scattering, was analyzed according to

$$\left[\frac{Kc}{\Delta R_\theta}\right]_{\theta=0} = \frac{1}{M_w} + 2A_2c + \dots \quad (1)$$

where the optical constant of the system K is defined as

$$K = \frac{2\pi^2 {n_B}^2 {i_B}\left(\frac{dn}{dc}\right)_\mu^2}{N_A\lambda^4 R_B} \quad (2)$$

with n_B and λ indicating the refractive index of benzene and the wavelength of the incident beam.

The number-average molecular weight, M_n, was determined by osmotic pressure measurements carried out with a Gonotech osmometer Osmomat 090 equipped with membranes with a cut off of 12 000.

6. Determination of Sugar Composition of Ulvan from U. Armoricana. The HPAEC chromatographic method coupled with a pulsed amperometric detector was used for this analysis. Determinations were carried out in the laboratories INRA, Nantes, according to the procedure reported by Quemener and Lahaye.[13]

Results of this determination are reported in Table 1.

7. Molecular Modeling. Molecular modeling calculations were performed on a Compaq Alpha XP1000 workstation with the CHARMm software package,[14−16] using version 22 parameters and partial charges. Nonbonding interactions were treated without a cutoff distance and the dielectric constant was fixed to 4. The hydrogen-bonding energy contribution was considered by appropriately adjusting the atomic partial charges and van der Waals parameters for hydrogen bond donor and acceptor atoms.[17] The carboxylic group of glucuronic and iduronic residues and the sulfate group on rhamnose were modeled as uncharged, by simulating a complete screening by counterions or a low-pH solution state. Force-field parameters for sulfate group were set accordingly to Huige and Altona.[18]

Cartesian coordinates were obtained by CHARMm considering glucuronic and rhamnose residues in $^4C_1$ and $^1C_4$ chair conformations, respectively. Internal coordinates data for sulfate group were derived from X-ray crystallographic data on sulfated carbohydrates.[19]

For iduronic residue both $^1C_4$ chair and $^2S_0$ skew boat conformations were considered, as the main contributors to the conformational equilibrium of the pyranose ring when α-L-idoA is an internal residue in oligo- or polysaccharide sequences.[20] This feature is also confirmed by the ^{1}H NMR coupling constant (J) values of vicinal protons obtained from studies on aldobiuronic sequences.[5,21] Iduronic residue in $^1C_4$ conformation was built by setting the ring dihedral angles to the corresponding values found for this uronic moiety in heparin oligosaccharide structures[22] whereas the $^2S_0$ skew boat conformation data were obtained by the crystal structure of methyl-2,3,4-tri-*O*-benzoyl-β-D-xylopyranoside.[23]

Energy maps as a function of the glycosidic dihedral angles were obtained for the disaccharides: β-D-glcpA-(1 → 4)-α-L-rhap 3-sulfate, α-L-rhap 3-sulfate-(1 → 4)-β-D-glcpA, α-L-idopA-(1 → 4)-α-L-rhap 3-sulfate, and α-L-rhap 3-sulfate-(1 → 4)-α-L-idopA, indicated hereafter as GR, RG, IR, and RI, respectively. Conformational space was explored by changing the dihedral angles ϕ [≡(H1−C1−O1−C4′)] and ψ [≡(C1−O1−C4′-H4′)], where the primes denote atoms of the residue at the reducing end, from −180° to 180° by increments of 20°. The rotational freedom of the carboxylic and sulfate groups was considered therefore, for each (ϕ, ψ) pair, the dihedral angle ω [≡(C4−C5−C6−O61)] of uronic residues and δ_1 [≡(C4−C3−OS1−S)] of rhamnose were independently varied by 20° from 0 to 180° and from −180° to 180°, respectively. The δ_2 [≡(C3−OS1−S −OS2)] dihedral of rhamnose was fixed to −60° as we verified that its variation has little influence on the disaccharide energy. The obtained energy dependence on δ_1 and δ_2 dihedral angles, defining the orientation of sulfate group on rhamnose, is in agreement with the results of a previous X-ray crystallographic and modeling investigation on sulfated carbohydrates.[19]

Rigid body energy maps were calculated for each of the six disaccharides, by considering, for a fixed (ϕ,ψ) geometry, the minimum energy structure in terms of ω and δ_1.

To evaluate the possible influence of the nearest-neighbor residues on the energy map of a disaccharide, we carried out a calculation on the GRGR tetramer by fixing in the minimum-energy conformation the GR glycosidic linkages and changing

Table 1. Sugar Composition of Ulvan from *U. Armoricana* Obtained from HPAEC Analysis

monosaccharide	% weight	% mol
Glc	1.8	2.5
Gal	2.0	2.8
Xyl	5.0	8.3
Rha	33.3	51.1
GlcA	17.3	19.9
IdoA	13.3	15.3
sulfate	26.7	*a*

[a] The amount of sulfated sugar determined independently is 64.9%.

the ϕ, ψ, ω, and δ_2 dihedral angles for the RG linkage. The resulting energy map does not significantly differ from that obtained for the corresponding disaccharide.

The helical fold of regular portions of ulvan chain, described as $(GR)_i$ or as $(IR)_i$ sequences, was calculated using a general method described in the literature.[24,25] The axial rise per disaccharide, *h*, and the number of disaccharide units per helical period, *n*, were derived from geometrical data relative to the position of four consecutive anomeric oxygen atoms of the oligosaccharide.

For the building up of the chain, only the (ϕ,ψ) pairs for the RG or RI glycosidic linkages were varied each time. The glycosidic dihedrals for the other linkages occurring in the segments, i.e., GR or IR, were confined to the corresponding minimum-energy values. The positions of the glycosidic oxygen atoms were then extracted and used to calculate *n* and *h* parameters for each conformation.

Results and Discussion

Regular arrangements of aldobiuronic sequences, namely sulfate glucuronorhamnose and sulfate iduronorhamnose, were suggested on the basis of an NMR study on enzymatically cleaved sequences.[5] Their extent in a ulvan chain is a matter of debate being easy to foresee a relation between the presence of these regular saccharidic blocks and the tendency of ulvan to form gels.

Circular Dichroism. A circular dichroic investigation on this issue was attempted on a sample of ulvan extracted from the seaweed *Ulva Rigida* and reported in a former paper by us.[11] The findings led us to support an essentially disordered conformation of the studied ulvan. In the present study we have tackled this aspect in further details on samples of ulvans from different types of *Ulva sp*.

For both acid and salt forms of ulvans, it was assumed a negligible contribution of the neutral sugars also present in the backbone to the dichroic signal ranging from 260 to 200 nm, where the main absorption is due to the n $\rightarrow \pi^*$ electronic transition of the carboxylic groups of the aldobiuronic moiety. The dichroic patterns were compared with weighted averages of the corresponding uronic acid methyl glycosides CD absorption available in the literature,[26] namely the β-D-methyl glucuronoside and the α-L-methyl iduronoside. In Figure 1a,b the CD spectra of UMV and of the separate contributions of the above-mentioned methylated uronic moieties in salt and acid forms are shown. The agreement between the observed CD spectra of the charged and uncharged forms of UMV, and a linear combination of the ellipticities of the corresponding methyled monosaccharides is satisfactory. This result is substantiated by the obtainment of a composition of uronic moieties that compares well with independent determinations carried out by HPAEC-PAD and *m*-hydroxybiphenyl assay, as is shown in Table 2.

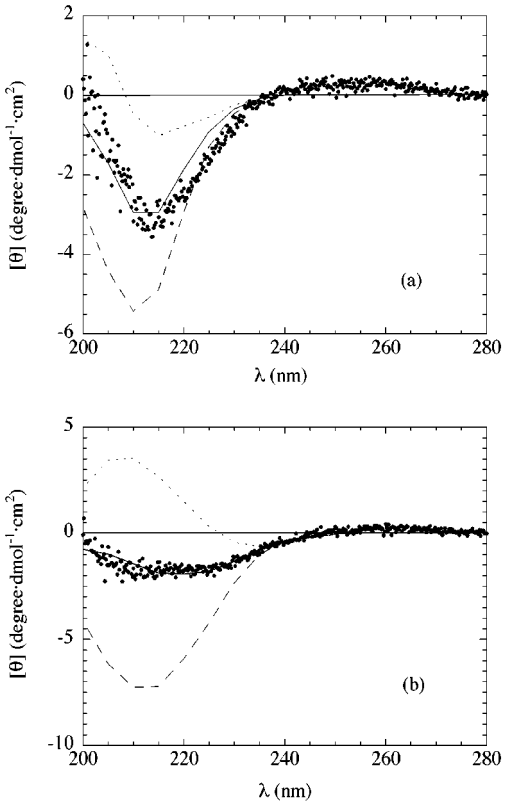

Figure 1. Circular dichroic spectra of ulvan in salt form (a) and in acid form (b): dotted line, glucuronic moiety contribution; dashed line, iduronic moiety contribution; solid line, linear combination of the two resulting contributions.

Table 2. Results from HPAEC-PAD, Circular Dichroism, and *m*-Hydroxybiphenyl Assay on the Aldobiuronic Composition of UMV[a]

method	% uronic acid	% GlucA	% IdoA
HPAEC-PAD	35.2	19.9	15.3
CD	34	18.4	15.6
m-hbp	37	n.a.	n.a.

Moreover, the simulation of the ellipticity of the acid and salt forms of UMV gave a consistent composition of iduronic and glucuronic residues for both the neutral and charged forms, i.e., 46% iduronic, 54% glucuronic and 50% iduronic, 50% glucuronic, respectively.

These results show that circular dichroism has some potentiality as a very simple method for the determination of the primary chemical composition of ulvan samples. On the other hand, it turned out that CD signal is not influenced by the presence of spatially limited ordered structures in the chain.

This method relies on quite substantial assumptions, i.e., a small contribution of neutral residues in the explored spectral range, identity of the conformational state of iduronic residue in the chain as well as methylated monosaccharide. Bearing in mind these considerations, we then used this approach exclusively as a characterization tool for the determination of the chemical composition of ulvans coming from different sources. The results of this analysis are summarized in Table 3.

In analogy with the case of UMV, the comparison of the circular dichroism spectra of ulvan from different sources with the corresponding methyl uronosides yielded the same composition for both the acidic and salt forms of ulvan. A variability in the uronic composition is detectable within the same algal source for ulvan from *Ulva Lactuca*.

Table 3. Composition of Uronic Moieties As Determined by Circular Dichroism

sample	source	% uronic moiety	% GlucA	% IdoA
UMV	*U. Armoricana*	34	54	46
ULM	*U. Lactuca*	34	80	20
URO	*U. Rotundata*	51	85	15
UBR	*U. Rigida* from Brittany	29	85	15
RIGIDA	*U. Rigida* from Venice lagoon	34	95	5
LACT 1	*U. Lactuca* (powdered or minced)	34	97	3

From Table 3 it is clear that UMV is the ulvan with the highest content of iduronic acid, in agreement with other works.[13] This feature increases the potentiality of the polysaccharide as substitute of heparin and heparin-like products.

Isothermal Microcalorimetry. A general behavior of charged regular polymers is the ability to bind oppositely charged species, i.e., metal ions or protons, and in favorable cases to undergo a conformational transition. A number of polysaccharides are known to display this behavior. Typically, the transition is entropy driven as a large number of water surrounding the saccharidic and metal ion charges are released upon the binding. Therefore, the study of the binding process of ulvan with some ionic species may reveal some degree of cooperativity related to a coupled conformational transition of the polysaccharide matrix.

Our UMV sample displayed the highest content of iduronic acid among the ulvan samples available. It is known[27] that this uronic moiety binds Cu(II) ions with higher affinity then the other carboxylated saccharidic residues present in the ulvan chain. Therefore, we investigated the binding of UMV with Cu(II) by microcalorimetry in order to ascertain the presence of an ordered conformation of the regular aldobiuronic sequences of ulvan in solution.

Isothermal microcalorimetry is a powerful approach for studying conformational rearrangements coupled with a binding process. A drawback of the method is that the monitored effect is relative to the overall heat evolved preventing the separation of the different contributions that occur in the binding. The association process in this case is further complicated by the presence of sulfate groups mainly of the rhamnose moiety which contribute to the association. Fortunately the binding constant of the sulfate groups is lower than that of the carboxylic moieties. The effective contribution of the former occurs only when the latter are almost saturated.

Any analysis of the binding curve is based on a model establishing a relationship between the free ligand and the macromolecule concentrations. When using microcalorimetry, the concentration of free ligand is not directly accessible.[28] In the absence of a conformational transition, this can be accessed by fitting the fractional binding, Θ, as a function of the total concentration, C_t, according to customary Langmuir adsorption process:

$$C_f = C_{tot} - \frac{1}{2}\left\{C_{tot} + M_{tot} + \frac{1}{K} - \left[\left(C_{tot} + M_{tot} + \frac{1}{K}\right)^2 - 4M_{tot}C_{tot}\right]^{1/2}\right\} \quad (3)$$

with

$$\Theta = \frac{KC_f}{1 + KC_f} \quad (4a)$$

This treatment on ulvan from *Ulva rigida* yielded an apparent binding constant[11] of 4000 M^{-1}. Taking into account that a disorder-to-order transition involves only the spatially regular blocks in the chain imparting an overall small cooperative effect to the binding process, a microcalorimetric isothermal titration of UMV with Cu(II), inset of Figure 2, was carried out with a polyelectrolyte concentration of 4.5×10^{-3} charge mol L^{-1} and determining an apparent binding constant equal to 17 000 M^{-1}. The higher value of K obtained for UMV respect to ulvan from *Ulva rigida* can be attributed to the larger content of IdoA present in UMV (see Table 3) as one of the uronic acids with higher affinity for copper ions.

With an estimate of the binding constant in dilute solution, we carried out a second titration with a concentration 5-fold higher in order to point out a cooperative binding behavior. In these conditions a small but detectable sigmoidal trend is present in the initial part of the direct binding curve. Assuming the overall apparent binding constant obtained from the titration of the dilute solution as independent from the concentration, we can evaluate the Cu(II) free ions concentration also in the titration of polymer at a concentration of 2.3×10^{-2} charge/L (Figure 2).

The evaluation of the cooperativity parameters can be achieved by means of the Monod−Wyman−Chageux binding model.[29] The assumptions of this model, hereafter called MWC, are as follows:

1. The polymer or, in our case, the regular blocks are made of a number N_T of equivalent units made of R residues less than or equal to n binding sites.

2. The N units can assume only two conformational states A and B. In the absence of ligand the equilibrium between the two states is governed by the constant $L^0 = N_B/N_A$.

3. The binding site, embedded in two different conformational states, has a different affinity for the ligand, expressed by the binding constants K_A and K_B, with $h = K_B/K_A$. The former rules the binding in the absence of the cooperativity effect.

The fractional binding of this model, Θ_{MWC}, is given by the equation

$$\Theta_{MWC} = \frac{z}{1+z}\frac{1 + L^0 h y^{n-1}}{1 + L^0 y^n} \quad (4b)$$

where z and y are defined as $z = K_A C_f$ and $y = (1 + hz)/(1 + z)$, respectively.

In the first term of eq 4b is recognizable the pure Langmuir binding mode on a monodimensional lattice, analogous to eq 2, whereas the second term introduces a sigmoidal trend to the binding curve.

As it is formulated, this model is somehow inadequate to the complex association pattern displayed by ulvan for the simultaneous presence of two uronic moieties with different affinities for Cu(II) ions, i.e., iduronic and glucuronic residues, and of a rhamnose sulfate moiety.

For this reason the fit obtained with the MWC model is satisfactory only in the first part of the Θ vs C_f binding curve where the contribution of the iduronic moiety is more relevant, obtaining the parameters shown in Table 4. With increasing fractional binding values the fit loses correlation with the experimental

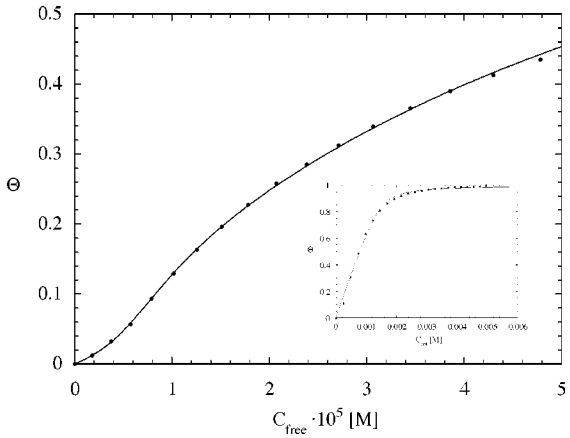

Figure 2. Fractional binding, Θ, as a function of the concentration of free Cu(II) ions in aqueous solution for a polymer concentration of 2.3×10^{-2} mol of charge/L. Inset: binding curve as a function of the total Cu(II) ions in solution for a polymer concentration of 4.5×10^{-3} M.

Table 4. Binding Parameters for the Cooperative Binding of Cu(II) Ions on UMV According to the Model (Eq 4b)

K_A (M^{-1})	17000 ± 700
K_B (M^{-1})	4500 ± 100
L^0	10 ± 4
n	37 ± 2

data, and unrealistic binding parameters are obtained. It should be taken into account that, after saturation of iduronic sites, the binding process progressively involves sites with minor affinity, i.e., glucuronic and sulfate rhamnose residues. The value of the parameter L^0 reflects the relative weight of the two conformations in which the binding site is distributed and shows that the less affine conformation for the binding is the more probable in the absence of ligand. This observation can be interpreted in the light of the capability of iduronic residues to assume in solution two ring arrangements, namely a $^1C_4$ chair and a $^2S_0$ skew boat conformation.[20] In this respect it is noteworthy to point out that (i) an NMR study carried out on aqueous solutions of iduronic residues containing oligosaccharides from heparin in the presence of different heavy metal ions[30] showed that the metal binding stabilizes the $^1C_4$ ring conformation and (ii) our previous Cu(II) binding study on a type of ulvan from *Ulva rigida* with a low content of iduronic residues (see Table 3) did not show any cooperativity.[11] From these considerations it can be inferred that the $^1C_4$ skew boat conformation of the iduronic moiety in the aldobiuronic sequences has a higher affinity for Cu(II) than the $^2S_0$ arrangement. The consequence of the capability of iduronic acid residues to switch between two different ring conformations is probably the cooperative effect found in the present study where an ulvan with high iduronic content has been examined. As will be shown in the modeling studies, this "local" feature of the residue can propagate in a more long-range distance scale.

Another clue on the conformational behavior of ulvan, opened by the Cu(II) association with UMV, was disclosed by the study of the neutralization enthalpy of UMV. In this case the isothermal titration microcalorimetry was used to monitor the heat effect during the titration of acid form of UMV with alkali. The neutralization reaction causes a changing of the charge density of the polyelectrolyte. This process can be coupled with a conformational change where the ordered structure

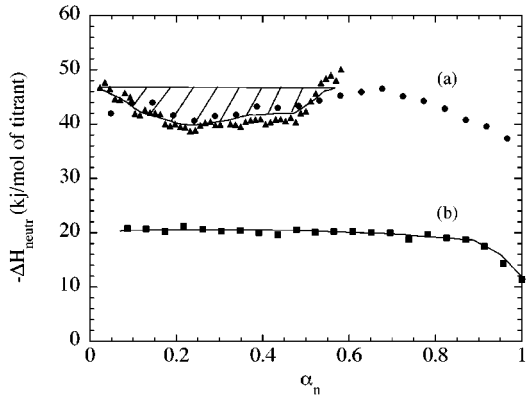

Figure 3. Enthalpy of neutralization vs degree of neutralization: (a) in the absence of ionic strength; (b) in the presence of ionic strength. Dashed area indicates an endothermic effect over the exothermic neutralization reaction.

present in the uncharged chain, i.e., the protoned form of ulvan, is replaced by a disordered state when a critical charge density is reached. In the literature it has been shown[31,32] that such behavior is easily recognizable by microcalorimetry in regularly sequenced polyelectrolytes as in the case of polypeptides. A less clear-cut situation is faced when the macroion is mainly formed by random sequences of residues with only few regular portions interspersed in the chain. In this case the overall exothermic enthalpy of neutralization will be partially decreased by an endothermic effect caused by the transition of the few ordered regions of the chains into a disordered state. The amount of this enthalpic effect as well as its detectability over the exothermic neutralization will be proportional to the extent of the regular regions of the polyelectrolyte. The experiments, shown in Figure 3, were carried out at different ulvan concentrations. In all cases a decrease of the neutralization heat was detected with a reasonable internal agreement, the limited ordered part of the backbone being made by the aldobiuronic sequences individuated by HPAEC methodology. To cross-check this interpretation, the same experiment was run in the presence of NaCl (0.1 M) as external ionic strength. A general lowering of the enthalpy of neutralization is obtained as expected, and the absence of the shallow minimum in the microcalorimetric titration confirms that the short regions are stabilized by the external electrolyte, in analogy with the behavior of other charged polysaccharides as carrageenans.[33] These findings although indirect suggest the capability of ulvan to assume ordered conformations in spatially limited portions of the chain. Such hypothesis was already proposed in a molecular dynamic simulation study of the pseudo-aldobiuronic unit.[34] An evaluation of the enthalpy of transition of the regular sequences corresponding to the dashed area indicated in Figure 3 leads to a value of about 2.3 kJ/mol of charge. As the aldobiuronic units bear two charges, an enthalpy effect of 4.6 kJ/aldobiuronic mol can be attributed to the order to disorder transition of the portions of chains where regular sequences of the aldobiuronic are present. If the structured conformation involves 1 hydrogen bond per aldobiuronic unit, as it turns out from conformational analysis of aldobiuronic chains, and considering its energy equal to 20 kJ/mol, an estimate of the amount of these units can be achieved. In our case this corresponds to about 20% of the total aldobiuronic units.

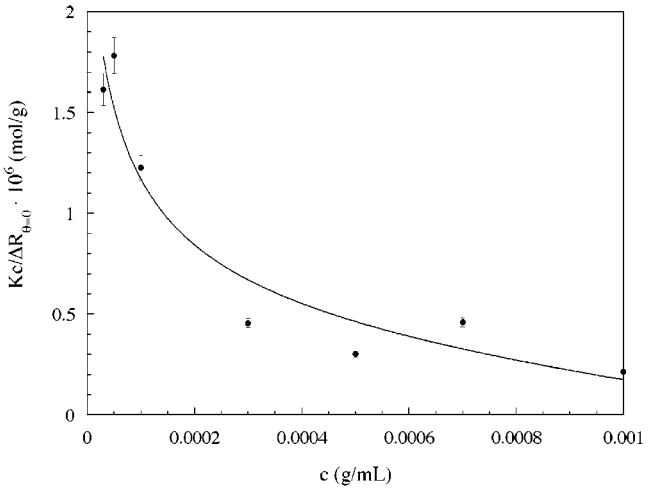

Figure 4. Forward scattering of 0.1 M NaCl aqueous solution at different concentrations of ulvan.

The partial ordering of the chain can also be related to the establishment of the junction zones of a macromolecular assembly responsible for the formation of the weak gel that ulvan is known to perform in nature.

The literature reports a very wide range of molecular weights of ulvan samples from 1.8×10^5 to 2×10^6 g/mol, mostly explainable as differences in the extraction/purification processes, polydispersity of the samples, variation of the characteristics of the samples depending on the seasonality of the crop. The self-associating tendency of this polysaccharide is also evidenced by the behavior of the light scattering of solution of ulvans in aqueous NaCl (0.1 M).

We have examined this latter characteristic on an ulvan UMV sample as a function of the concentration. The forward scattering as a function of the concentration yields a negative second virial coefficient in the presence of NaCl (0.1 M) for concentrations ranging from 0.03 to 1 g/L. The trend of the $Kc/\Delta R_{\theta\to 0}$ values shown in Figure 4 indicates an open association of chains since a critical concentration revealing a stoichiometry in the aggregation is not found. According to the association/aggregation theory worked out by Elias and Lys,[35,36] an average association constant can be extracted from the data.

Assuming that all the aggregation steps from unimer to multimer formation have the same equilibrium constant in Θ conditions, it is possible to describe the observed weight-average molecular weight as a function of the concentration expressed in g/mL as is indicated by eq 5:

$$(M_w)_{obs}{}^2 = (M_w)_I{}^2 + 4000({}^nK_0)\left[\frac{(M_w)_I{}^2}{(M_n)_I}\right]c \qquad (5)$$

The weight-average molecular weight of the unimer, $(M_w)_I$, forming the macromolecular assembly can be evaluated along with the average aggregation constant, ${}^nK_0$, expressed on molar scale by combining eq 5 with the usual dependence of the forward scattering, eq 1:

$$\frac{Kc}{\Delta R_{\theta=0}} = \left[(M_w)_I{}^2 + 4000({}^nK_0)\left[\frac{(M_w)_I{}^2}{(M_n)_I}\right]c\right]^{-1/2} + 2A_2c \qquad (6)$$

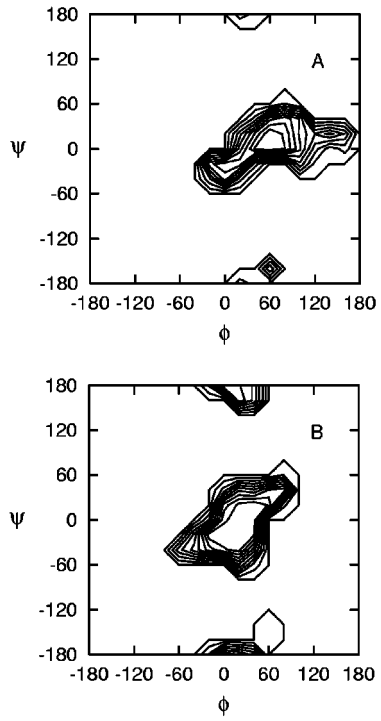

Figure 5. Energy maps of ulvan disaccharides. GR (A) and RG (B). Contours are separated by 2 kcal/mol levels.

where A_2 has the usual meaning and $(M_n)_I$ is the number-average molecular weight of the unimer.

Using the fitting eq 6 for the forward scattering as a function of the concentration, a value of about 4×10^5 g/mol for $(M_w)_I$, an average aggregation constant ${}^nK_0$ of 1.2×10^6 M^{-1} and a second virial coefficient A_2 of -1.2×10^{-4} mol mL g^{-2} were obtained. A value of 1.3×10^5 for $(M_n)_I$ determined independently by osmometry has been used in the data treatment.

The aggregation phenomena evidenced in this study offer a possible explanation for the large dispersity of the molecular weight values obtained by means of different techniques in the literature. It can be expected that, besides the dependency of the measurements on the purification treatment adopted in these works, the results so far collected are most likely dependent on the concentration range selected for the measurement. This situation cause large differences in the evaluation of the molecular weight.

A conformational study of the glycosidic linkages involving uronic residues in ulvan was carried out in a molecular modeling study.

The energy maps calculated for GR, RG, IR, and RI disaccharides are shown in Figure 5 and Figure 6. The minimum-energy conformers are described in Table 5. The low-energy (ϕ,ψ) region obtained for GR is in agreement with that explored by the β-D-glcpA-(1 → 4)-α-L-rhap disaccharide in a reported molecular dynamics simulation.[34] Moreover, the α-L-idopA2(OSO_3)−(1 → 4)-α-glcpNSO_3,6(OSO_3) heparin disaccharide has the same glycosidic linkage topology of RG in ulvan. The values of the glycosidic dihedral angles for this linkage in known crystal and solution structures of heparin[22,37] fall in the minimum-energy region found in our analysis.

From an inspection of Figures 5 and 6, it can be noted that the disaccharides with the uronic residue at the nonreducing end are confined in a smaller (ϕ,ψ) conformational space than the corresponding disaccharides with the uronic moiety at the reducing end.

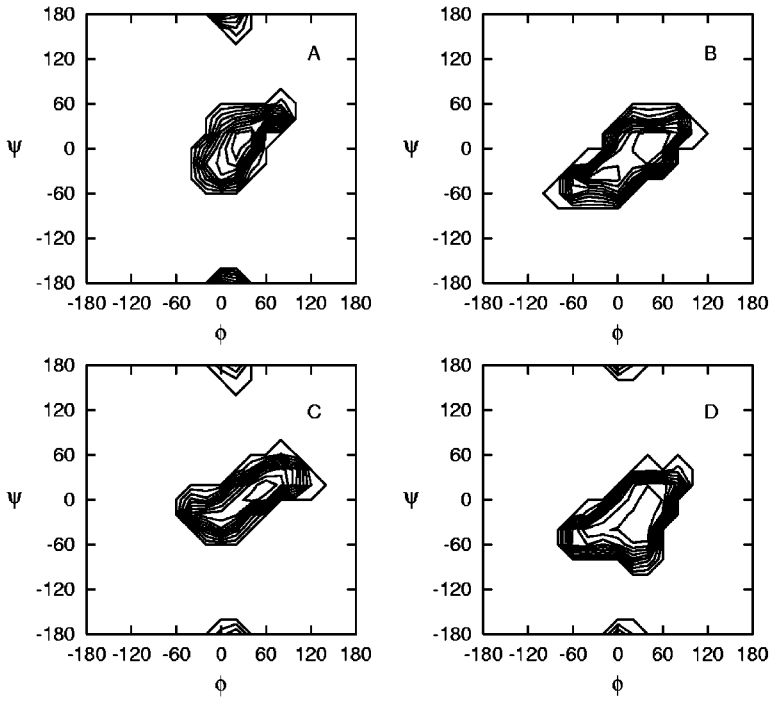

Figure 6. Energy maps of ulvan disaccharides: IR with iduronic in the $^1C_4$ conformation (A); RI with iduronic in the $^1C_4$ conformation (B); IR with iduronic in the $^2S_0$ conformation (C); RI with iduronic in the $^2S_0$ conformation (D). Contours are separated by 2 kcal/mol levels.

Table 5. Minimum-Energy Structures for Aldobiuronic Disaccharides

disaccharide	ring conformations	glycosidic linkage geometry	ϕ (deg)	ψ (deg)
G → R	$^4C_1 \rightarrow {}^1C_4$	eq−eq	60	20
R → G	$^1C_4 \rightarrow {}^4C_1$	ax−eq	40	20
I → R	$^1C_4 \rightarrow {}^1C_4$	ax−eq	40	20
R → I	$^1C_4 \rightarrow {}^1C_4$	ax−ax	40	0
			−20	−40
I → R	$^2S_0 \rightarrow {}^1C_4$	ax−eq	60	20
R → I	$^1C_4 \rightarrow {}^2S_0$	ax−ax	40	−40

The minimum-energy structures of GR and IR denote that the hydroxyl group on C2 of the uronic residue and an oxygen atom belonging to the sulfate group on C3 of rhamnose face on the same side at a distance compatible with the setting of a hydrogen bond.

For RG and RI disaccharides we found that conformers with energy within 2 kcal/mol from the main minimum can differ in ϕ and ψ up to 40°, with a consequent higher conformational freedom for these linkages. The populated structures show the sulfate group of rhamnose and the carboxylic group of the uronic residue arranged on the same side of the glycosidic linkage, with the possible setting of a hydrogen bond involving atoms of the two groups.

In G → R → G or I → R → I sequences with glycosidic linkages in the most stable conformations, oxygen atoms of the rhamnose sulfate group can interact via hydrogen bond with the hydroxyl group on C2 of the preceding uronic residue or alternatively with the carboxylic oxygen of the following uronic residue. By considering a regular segment of alternated G and R or I and R residues, a network of consecutive, although not simultaneous, hydrogen bonds stabilizes the ordered chain conformation, with an average number of hydrogen bonds per aldobiuronic unit equal to 1.

To consider the topology of possible secondary structures, we studied the helical fold of models of ulvan chain, described as a regular sequence of G → R or I → R dimers, corresponding to the A_{3S} and B_{3S} nomenclature adopted by Lahaye.[5]

The possible families of helices as a function of the glycosidic linkages geometry were obtained in the following way. The ϕ and ψ angles of the G → R or I → R glycosidic linkages were set to the corresponding minimum-energy values (see Table 5), and the values of R → G or R → I glycosidic dihedral angles were systematically varied to obtain the related topologies for chain segments.

The values of n (number of dimers per helical period) and h (axial rise per dimer) were calculated in the vicinity of the energy minima reported in Figure 5B and Figure 6B,D. According to this analysis for the G → R sequence, in the region of ϕ and ψ values entailed within 2 kcal/mol of the conformational minimum, left-handed helices were found with n ranging from 3 to 5 dimers per helical period and corresponding to a number of helical turns from 2 to 4, respectively. The resulting chains are highly extended structures with a rise per residue, h, larger than 9 Å, where $h = 9.9$ Å is the value for the fully stretched topology.

The overall shape of the I → R sequences depends on the iduronic ring conformation. For iduronic residues in $^1C_4$ conformation the analysis showed the existence of two conformations with almost the same energy, as indicated in Figure 6B. Considering the larger minimum region ($\phi = 60°$ and $\psi = 0°$), left-handed 4-fold helices with a value of h of about 7.4 Å are obtained. A more elongated trans arrangement with h around 8.4 Å pertains to the minimum characterized by a smaller ϕ, ψ range.

For the IR sequences with iduronic residues in the $^2S_0$ conformation, only extended low-symmetry left helices are found, with 2.5 dimers per repeat in 1.5 helix turns and a rise per dimer of 8.4 Å.

The three aldobiuronic sequences considered are shown in Figure 7. It is noteworthy to point out the more

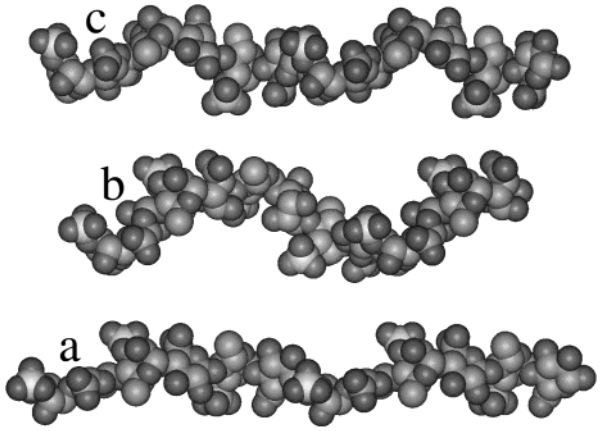

Figure 7. Models of aldobiuronic chains: A_{3S} chain (a); B_{3S} chain with iduronic in the $^1C_4$ conformation (b); B_{3S} chain with iduronic in the $^2S_0$ conformation (c).

folded arrangement adopted by the B_{3S} chain where the iduronic ring is in the $^1C_4$ conformation.

Concluding Remarks

Ulvan is a polysaccharide obtained from an algal low-cost biomass. Its exploitation for innovative uses in fields such as pharmaceutics or food is related to the conformational properties displayed in solution. In this respect the ability to form weak gels in the presence of ionic species, the presence of rare sugars such as iduronic acid and rhamnose in the regular sequences of the polysaccharide backbone make this biopolymer an interesting subject of investigation. The study presented in this paper points out that the regular sequences of ulvan can undergo an order → disorder conformational transition. This process is probably triggered by the ring conformational equilibrium of L-iduronic acid moiety involving $^2S_0$ and $^1C_4$ arrangements and by the setting up of one intramolecular hydrogen per aldobiuronic unit. It is also noteworthy the aggregating tendency of this polysaccharide in dilute aqueous solutions in the presence of 0.1 M NaCl.

This study showed that circular dichroism is not capable of detecting structural changes promoted by ligand binding and involving short portions of the overall chain. On the other hand, isothermal microcalorimetry can be suitably used as a methodology to study the energetics of both the binding and order → disorder processes.

It is clear that the conformational features of ulvan pointed out in this work need further investigation for obtaining a formulation of innovative application of this product from algal biomass.

Acknowledgment. F.C. was the recipient of a "Short Term Mission" within the frame of the action P1 "Physics of Soft Matter" of the European COST program. We acknowledge with thanks Dr. Quemener for assistance in carrying out the HPAEC measurements.

References and Notes

(1) *Seaweed Resources in Europe: Uses and Potential;* Guiry, M. D., Blunden, G., Eds.; John Wiley and Sons: New York, 1991.
(2) Percival, E. *Br. Phycol. J.* **1979**, *14*, 103−117.
(3) Percival, E.; Wold, J. K. *J. Chem. Soc.* **1963**, 5459−5468.
(4) Lahaye, M.; Inizan, F.; Vigouroux, J. *Carbohydr. Polym.* **1998**, *36*, 239−249.
(5) Lahaye, M.; Brunel, M.; Bonnin, E. *Carbohydr. Res.* **1997**, *304*, 325−333.
(6) Perlin, A. S.; Mackie, D. M.; Dietrich, C. P. *Carbohydr. Res.* **1971**, 185−194.
(7) Alban, S.; Schauerte, A.; Franz, G. *Carbohydr. Polym.* **2002**, *47*, 267−276.
(8) Bobin-Dubigeon, C.; Lahaye, M.; Guillon, F.; Barry, J. L.; Gallant, D. *J. Sci. Food. Agric.* **1997**, *75*, 341−351.
(9) Haug, A. *Acta Chem. Scand.* **1976**, *b30*, 562−566.
(10) Lahaye, M.; Axelos, M. A. V. *Carbohydr. Polym.* **1993**, *22*, 261−265.
(11) Paradossi, G.; Cavalieri, F.; Pizzofzerrato, L.; Liquori, A. M. *Int. J. Biol. Macromol.* **1999**, *25*, 309−315.
(12) Viebke, C. *Carbohydr. Polym.* **1995**, *28*, 101−105.
(13) Quemener, B.; Lahaye, M.; Bobin-Dubigeon, C. *J. Appl. Phys.* **1997**, *9*, 179−188.
(14) Brooks, B. R.; Bruccolieri, R. E.; Olafson, B. D.; States, D. J.; Swaminathan, S.; Karplus, M. *J. Comput. Chem.* **1983**, *4*, 187−217.
(15) Smith, J. C.; Karplus, M. *J. Am. Chem. Soc.* **1992**, *114*, 801−812.
(16) Schmidt, J. M.; Brüschweiler, R.; Ernst, R. R.; Dunbrack, R. L., Jr.; Joseph, D.; Karplus, M. *J. Am. Chem. Soc.* **1993**, *115*, 8747−8756.
(17) Brady, J. W.; Schmidt, R. K. *J. Phys. Chem.* **1993**, *97*, 958−966.
(18) Huige, C. J. M.; Altona, C. *J. Comput. Chem.* **1995**, *16*, 56−79.
(19) Lamba, D.; Glover, S.; Mackie, W.; Rashid, A.; Sheldrick, B.; Pèrez, S. *Glycobiology* **1994**, *4*, 151−163.
(20) Ferro, D. R.; Provasoli, A.; Ragazzi, M.; Casu, B.; Torri, G.; Bossennec, V.; Perly, B.; Sinay, P.; Petitou, M.; Choay, J. *Carbohydr. Res.* **1990**, *195*, 157−167.
(21) Venkataraman, G.; Sasisekharan, V.; Cooney, C. L.; Langer, R.; Sasisekharan, R. *Proc. Natl. Acad. Sci. U.S.A.* **1994**, *91*, 6171−6175.
(22) Faham, S.; Hileman, R. E.; Fromm, J. R.; Linhardt, R. J.; Rees, D. C. *Science* **1996**, *271*, 1116−1120.
(23) Vangehr, K.; Luger, P.; Paulsen, H. *Chem. Ber.* **1980**, *113*, 2609−2615.
(24) Miyazawa, T. *J. Polym. Sci.* **1961**, *55*, 215−231.
(25) Sugeta, H.; Miyazawa, T. *Biopolymers* **1967**, *5*, 673−679.
(26) Morris, E. R.; Rees, D. A.; Sanderson, G. R.; Thom, D. *J. Chem. Soc., Perkin Trans. 2* **1975**, 1418−1425.
(27) Whitfield, D. M.; Sarkar, B. *J. Inorg. Biochem.* **1991**, *41*, 157−170.
(28) Wiseman, T.; Williston, S.; Brandts, J. F.; Lin, L. N. *Anal. Biochem.* **1989**, *179*, 131−137.
(29) Cantor, C. R.; Schimmel, P. R. *Biophysical Chemistry*; Freeman Co.: San Francisco, CA, 1980; Part III, Chapter 17.
(30) Whitfield, D. M.; Choay, J.; Sarkar, B. *Biopolymers* **1992**, *32*, 585−596.
(31) Rialdi, G.; Hermans, J. Jr. *J. Am. Chem. Soc.* **1966**, *88*, 5719−5726.
(32) Chou, P. Y.; Scheraga, H. A. *Biopolymers* **1971**, *10*, 657−680.
(33) Norton, I. T.; Goodall, D. M.; Morris, E. R.; Rees, D. A. *J. Chem. Soc., Faraday Trans.* **1983**, *79*, 2475−2488.
(34) You, L.; Shi, Y.; Wang, C.; Lahaye, M.; Tran, V. *Chem. Phys.* **1997**, *224*, 81−94.
(35) Elias, H. G.; Lys, H. *Makromol. Chem.* **1966**, *96*, 64−82.
(36) Elias, H.-G. In *Light Scattering from Polymer Solutions*; Huglin, M. B., Ed.; John Wiley and Sons: New York, 197.
(37) Mulloy, B.; Forster, M. J.; Jones, C.; Davies, D. B. *Biochem. J.* **1993**, *293*, 849−858.

MA020134S